UCLA
UCLA Previously Published Works

Title

Using iPSC-derived neurons to uncover cellular phenotypes associated with Timothy syndrome

Permalink

https://escholarship.org/uc/item/6kj514gz

Journal

Nature Medicine, 17(12)

ISSN

1078-8956

Authors

Paşca, Sergiu P
Portmann, Thomas
Voineagu, Irina
et al.

Publication Date

2011-12-01

DOI

10.1038/nm.2576

Peer reviewed

Using iPS cell-derived neurons to uncover cellular phenotypes associated with Timothy Syndrome

Sergiu P. Paşca[1], **Thomas Portmann**[1,*], **Irina Voineagu**[2,*], **Masayuki Yazawa**[1,*], **Oleksandr Shcheglovitov**[1], **Anca M. Paşca**[1], **Branden Cord**[3], **Theo D. Palmer**[3], **Sachiko Chikahisa**[4], **Nishino Seiji**[4], **Jonathan A. Bernstein**[5], **Joachim Hallmayer**[4], **Daniel H. Geschwind**[2], and **Ricardo E. Dolmetsch**[1]

[1]Department of Neurobiology, Stanford University School of Medicine, Stanford, California, USA

[2]Department of Psychiatry and Biobehavioral Sciences, David Geffen School of Medicine, University of California, Los Angeles, California, USA

[3]Department of Neurology, Stanford University School of Medicine, Stanford, California, USA

[4]Department of Psychiatry & Behavioral Science, Stanford University School of Medicine, Stanford, California, USA

[5]Department of Pediatrics, Stanford University School of Medicine, Stanford, California, USA

Abstract

Monogenic neurodevelopmental disorders provide key insights into the pathogenesis of disease and help us understand how specific genes control the development of the human brain. Timothy syndrome is caused by a missense mutation in the L-type calcium channel $Ca_v1.2$ that is associated with developmental delay and autism [1]. We generated cortical neuronal precursor cells and neurons from induced pluripotent stem cells derived from individuals with Timothy syndrome. Cells from these individuals have defects in calcium (Ca^{2+}) signaling and activity-dependent gene expression. They also show abnormalities in differentiation, including decreased expression of genes that are expressed in lower cortical layers and in callosal projection neurons. In addition, neurons derived from individuals with Timothy syndrome show abnormal expression of tyrosine hydroxylase and increased production of norepinephrine and dopamine. This phenotype can be reversed by treatment with roscovitine, a cyclin-dependent kinase inhibitor and atypical L-type–channel blocker [2, 3, 4]. These findings provide strong evidence that $Ca_v1.2$

Correspondence to: Ricardo E. Dolmetsch, Department of Neurobiology, 299 Campus Drive, Stanford CA 94305, ricardo.dolmetsch@stanford.edu, Tel: (650) 723 9812.
*Contributed equally to this work

regulates the differentiation of cortical neurons in humans and offer new insights into the causes of autism in individuals with Timothy syndrome.

Human genetic studies have implicated voltage-gated calcium channels, in particular the L-type channel $Ca_V1.2$, in the development of psychiatric diseases such as autism[5], bipolar disorder[6] and schizophrenia[7]. Although calcium influx through these channels is important for a variety of neuronal processes including regulation of gene expression[8], the cellular defects caused by mutations in these channels and how these defects lead to psychiatric symptoms is unknown. TS is caused by a point mutation in an alternatively spliced exon of *CACNA1C*, the gene that encodes the α_1 subunit of $Ca_V1.2$[1]. This mutation leads to decreased calcium- and voltage-dependent inactivation of the channel[1,9]. TS patients suffer from cardiac arrhythmia, hypoglycemia and global developmental delay. Over 60% of TS patients also fulfill the criteria for an autism spectrum disorder (ASD)[1] making TS one of the most penetrant monogenic forms of autism.

To determine the cellular consequences of the TS mutation, we used somatic cell reprogramming[10,11] to generate iPSCs from individuals with TS (see Supplementary Figs. 1, 2, Methods and reference[12] for characterization, and Supplementary Table 1 for a list of lines). We differentiated the iPSC lines into NPCs and neurons using conditions that favor the generation of cortical neurons[13–15] (Fig. 1, Supplementary Fig. 3, and Methods for details on differentiation). To identify the types of cells in these cultures, we used Fluidigm Dynamic Arrays[16] to measure the expression of region and cell-type specific marker genes in single cells (Fig. 1b; see Supplementary Table 2). The reliability and accuracy of this method for measuring single cell gene expression was verified in a variety of ways (see[17], Supplementary Figs. 4, 5 and Methods). Overall, 64.9% of the cells at day 45 of differentiation *in vitro* expressed a neuronal marker (*MAP2* or *NCAM*), and 76% of these cells were positive for the early neuronal marker Doublecortin (*DCX*)[18]. Individual neurons expressed combinations of genes that could be used to determine their neurotransmitter identity and cortical layer specificity (Fig. 1b lower). A substantial number of neurons expressed excitatory markers like *VGLUT1* and *VGLUT2* along with the dopamine receptor *DRD2*, whereas others expressed the inhibitory markers *GAD65*, *GAD67* and *VGAT*.

The expression of *FOXP1*, *ETV1*, *SATB2*, *CTIP2*, *CUX1* and *RELN* was used to define cortical layer identity, based on immunohistochemical analysis of human brains[19,20] (Fig. 1c). Ninety-one percent of the NCAM+ neurons expressed at least one cortical layer marker. The expression of *ETV1* and *FOXP1* was used to indicate a lower cortical layer identity, while the expression of *CUX1*, *SATB2*, *CTIP2* and *RELN* in the absence of *ETV1* and *FOXP1* was used to define upper layer neurons. Approximately 85% of cortical neurons could be classified as lower layer neurons while the remaining 15% expressed markers of upper cortical layers (Fig. 1d). Among the lower layer neurons we could identify two distinct subpopulations (Fig. 1e): cells expressing *CTIP2*, which defines a population of subcortical projection neurons, and cells expressing *SATB2*, which defines neurons that project to distant cortical regions via the corpus callosum[21–23].

A notable finding from this analysis was the remarkable reproducibility of the neuronal differentiation protocol across multiple iPSC lines and individuals (average standard

deviation for the proportion of cells expressing a particular marker was 4.47%), indicating that single cell analysis of gene expression is reproducible and can be used to identify defects in neuronal differentiation.

The ability to generate well-defined populations of NPCs and neurons from iPSCs prompted us to ask whether we could identify cellular phenotypes associated with TS. We examined the proliferation (Supplementary Fig. 6a) and migration of NPCs (Supplementary Fig. 6b,c) and the total number of neurons generated (Supplementary Fig. 5), but found no differences between controls and TS cultures. We next used patch clamp recording and calcium imaging to assess the physiological properties of the neurons generated from iPSC lines (Fig. 1f). We found that 57% of the iPSC-derived cells fired mature action potentials (APs) (Supplementary Fig. 7). Comparison of TS and control neurons did not reveal any significant differences in AP threshold or amplitude, resting membrane potential, input resistance or capacitance (Supplementary Table 3). However, the APs of TS neurons were approximately 37% wider at the midpoint than those of controls (TS: 3.92 ± 0.49 versus Ctrl: 2.86 ± 0.12 ms, $P = 0.008$), which is consistent with a loss of channel inactivation (Fig. 1f,g) and is similar to the defect we observed in TS-derived cardiomyocytes[12].

We next examined intracellular calcium ($[Ca^{2+}]_i$) signals in TS and control NPCs and neurons using Fura-2 and time-lapse video microscopy. Because the cultures contain a mixed population of neurons and NPCs, we first measured $[Ca^{2+}]_i$ in mature neurons expressing a YFP reporter gene under the control of the Synapsin-1 promoter (Fig. 1h). In TS cells we observed a significant increase in the sustained $[Ca^{2+}]_i$ rise following depolarization that was abolished by treatment with nimodipine (Fig. 1i). This increased $[Ca^{2+}]_i$ rise in TS neurons was observed in neurons derived from multiple lines and multiple independent differentiations (Supplementary Fig. 8a,b, Fig. 1j). Similarly, increased $[Ca^{2+}]_i$ elevations were observed in TS-derived NPCs (Supplementary Fig. 8c,d). Taken together, these results provide strong evidence that NPCs and neurons derived from TS individuals have defects in AP firing and $[Ca^{2+}]_I$ signaling.

$Ca_V1.2$ plays an important role in regulating activity-dependent gene expression in the nervous system[8]. We therefore used Illumina microarrays to compare the gene expression profile of TS and control NPCs and neurons (Fig. 2a–d). Hierarchical clustering based on differentially expressed genes showed that TS-derived cells clustered separately from controls. The expression levels of 211 genes in neurons (126 upregulated, 85 downregulated) and 136 genes in NPCs (58 upregulated, 78 downregulated) were significantly altered in TS cells (Fig. 2c,d and Supplementary Table 4). Of the genes that were altered in TS neurons, 11 have been previously implicated in either ASD or intellectual disability (ID)[24,25] (Supplementary Table 5).

We also identified 223 genes (135 upregulated, 88 downregulated) that were altered in TS relative to control neurons upon depolarization. A number of the genes that were altered in TS cells are linked to Ca^{2+}-dependent regulation of the transcription factor CREB (Fig. 2e,f) including *RSK*/*MSK* and *CAMKII*. Others such as *EGR1*, *FOS*, *FOSB*, *GAD67* and *TH* are downstream targets of *CREB*. In addition to *TH*, which is the rate-limiting enzyme in the production of dopamine and norepinephrine, *DRD1IP* (Calcyon), another gene involved in

dopamine signaling, was also upregulated in TS neurons. These results suggest that the TS mutation leads to misregulation of Ca^{2+}-dependent gene expression and perturbs catecholamine signaling.

To determine whether the TS mutation leads to defects in neuronal differentiation, we used Fluidigm Arrays to study the identity of cells generated from individuals with TS versus controls (Fig. 3a). We found a significant decrease in the fraction of neurons expressing lower layer markers in TS relative to controls (TS: 66.7% versus Ctrl: 85.5%, $P < 0.001$; Fig. 3b), and an increase in the fraction of neurons expressing upper layer markers (TS: 33.3% versus Ctrl: 14.5%, $P = 0.002$; Fig. 3b). TS cells expressing lower layer markers cells (Fig. 3c) contained a significantly lower proportion of *SATB2* expressing cells (TS: 31.0% versus Ctrl: 55.3%, $P < 0.001$) and an increase in *CTIP2* expressing cells (TS: 8.0% versus Ctrl: 1.0%, $P = 0.01$). Because *SATB2* is both necessary and sufficient for the formation of callosal projection neurons[21,22], this finding is consistent with the notion that the TS mutation decreases the fraction of callosal projection neurons and increases the number of cells that project to subcortical structures.

To validate these findings *in vivo* we also measured Satb2 expression in a transgenic mouse expressing the TS channel driven by the *Foxg1* promoter in the forebrain (Supplementary Fig. 9). TS transgenic mice had a reduced number of Satb2 expressing cells that was most pronounced in lower layers (Fig. 3d–f), whereas Foxp1 expression (Fig. 3g) and the total number of NeuN expressing neurons in the cortex were unchanged. We therefore conclude that the TS mutation alters *SATB2* expression both *in vitro* and *in vivo*. Interestingly, we did not observe an increase in the number of Ctip2 expressing cells in the TS channel-expressing mice. This could be either because of differences between *in vivo* and *in vitro* neuronal differentiation or because of species-specific differences in Ctip2 regulation. CTIP2 is in fact expressed more broadly in humans, labeling cells in the subventricular zone as well as in cortical layers II and V[26].

We also observed a significant increase in the fraction of cells that expressed *TH* in TS-derived neuronal cultures (TS: 16.4% versus Ctrl: 8.0%, $P = 0.03$; Fig. 3a). This agrees with our earlier finding that genes involved in catecholamine synthesis are misregulated in TS. To determine whether the TS mutation alters the regulation of *TH*, we measured *TH* mRNA in TS and control neurons following electrical activation (Fig. 4a). After nine hours of stimulation, *TH* was downregulated in control neurons but upregulated in TS neurons, indicating that the TS mutation prevents down-regulation of TH in response to prolonged electrical activity. To provide evidence that this increase in *TH* mRNA has functional consequences we measured expression of TH protein using a TH specific antibody. We found that TS neuronal cultures contained 6.3 times more TH^+ neurons ($TH^+/MAP2^+$ cells) than control cultures (Fig. 4b–d; TS: 15.03% ± 0.92%, $n = 9$ differentiations; Ctrl: 2.52% ± 0.62%, $n = 7$ differentiations; t-test, $P < 0.001$ or than cultures generated from an individual with 22q11.2 deletion syndrome, another neurodevelopmental disorder (Fig. 4c). To determine whether this change in TH protein caused an increase in the production of catecholamines, we used high-pressure liquid chromatography (HPLC) to measure the level of norepinephrine and dopamine in the media collected from neuronal cultures. We found that the TS neurons secreted 3.5 times more norepinephrine (TS: $34.7 \pm 4.02 \times 10^{-5}$ versus

Ctrl: $9.79 \pm 1.83 \times 10^{-5}$ pg μl^{-1} neuron^{-1}, t-test, $P = 0.004$) and 2.3 times more dopamine (TS: $4.56 \pm 0.36 \times 10^{-5}$ versus Ctrl: $2.05 \pm 0.24 \times 10^{-5}$ pg μl^{-1} neuron^{-1}, t-test, $P = 0.001$) than control lines, strongly suggesting that the TS mutation leads to increased TH expression and to an excess secretion of catecholamines (Fig. 4e).

We next investigated the cellular identity of neurons that produce TH in TS and control cultures. In both control and TS cultures, TH expressing neurons were not stained with antibodies to FOXA2 or EN1, markers of midbrain neurons, or GABA, a marker for dopaminergic olfactory neurons in the forebrain (Fig. 4f). Using Fluidigm chip analysis we found that TH expression was not confined to any specific class of neurons, although these cells were more likely to co-express excitatory markers and dopamine-related genes (Fig. 4g). This suggests that the TS channel does not promote a catecholaminergic cell fate, but instead increases the expression of TH in a variety of cortical cell types. Interestingly, we did not observe an increase in TH staining in the cortex of transgenic mice expressing the TS channel. This likely reflects the low homology between the promoter regions of the mouse and human *TH* genes and differences in gene regulation[27,28].

Finally, to determine if the increase in TH expression in TS neurons was reversible and a result of L-type channel activity, we treated 39 day-old neurons from TS individuals with L-type channel blockers. The conventional L-type calcium channel blocker nimodipine failed to reverse the excess expression of TH in these neurons. Earlier studies in cardiomyocytes[12] from TS individuals indicated that roscovitine[2,3,29], a cyclin-dependent kinase blocker that also increases L-type channel inactivation, can reduce the prolongation of the cardiac AP in cells from TS individuals. Treatment with roscovitine caused a 68% reduction in the proportion of TH^{+} neurons (Fig. 4h,i; two-way ANOVA, $P < 0.01$, $n = 3,975$ neurons from three TS lines and $n = 2,679$ from three control lines) without affecting the fraction of MAP2 expressing cells. This result suggests that the increase in TH expression probably results from lack of inactivation of the TS channels and, further, that restoring channel inactivation in mature neurons can decrease the abnormal expression of TH in patient cells.

In this study we show that neurons from patient-derived iPSCs can be used to identify cellular phenotypes associated with a neurodevelopmental disorder. These findings provide insight both into the function of Ca$_{v}$1.2 in the developing human brain and its role in the pathogenesis of psychiatric diseases. We report an increase in the amplitude of Ca^{2+} elevations in TS derived NPCs and neurons indicating that loss of inactivation in a single splice variant of Ca$_{v}$1.2 can have profound effects on neuronal signaling. A consequence of this defect was a change in activity-dependent gene expression and an increase in cells producing norepinephrine and dopamine, consistent with previous experiments showing that dopaminergic specification is activity dependent[39]. The TS mutation also caused a decrease in neurons expressing *SATB2*, a marker for callosal projection neurons. This finding is unexpected because Ca$_{v}$1.2 has not been previously linked to the specification of these cells. The increase in *SATB2* expressing cells was recapitulated in the cortex of a mouse expressing the TS channel. However, this mouse did not show an increase in TH expression probably reflecting species-specific differences in gene regulation and the structure of the TH promoter[27,28].

A key question is whether these cellular defects help to explain developmental delay and ASD in individuals with TS. The reduction in cortical projecting neurons in TS is consistent with the emerging view that ASDs arise from defects in connectivity between cortical areas[30,31], and agrees with studies that show a decreased size of the corpus callosum in ASD[32]. Ectopic production of TH and a subsequent increase in catecholamine synthesis agrees with findings from valproic-acid based models of ASD[33] and postmortem studies of patients with schizophrenia[34]. As catecholamines play an important role in sensory gating and in social behavior, an increase in their synthesis might be important in the pathophysiology of ASDs.

ONLINE MATERIALS AND METHODS

iPSC maintenance

Human iPSCs and the embryonic H9 line were cultured on irradiated DR4 mouse embryonic fibroblast feeders.

Neural differentiation protocol

Neural differentiation was carried out using a modified version of a previously described protocol[13]. Briefly, the iPSCs were suspended to generate embryoid bodies (EBs) and plated to produce neural rosettes (Fig. 1a **upper**). The rosettes were mechanically isolated and expanded as neurospheres, and then either purified by fluorescence activated cell sorting (FACS) using the forebrain progenitor marker FORSE-1[35,36] or plated for differentiation into neurons. Seven days after plating of the neurospheres, MAP2ab positive cells were observed migrating away from radial clusters of undifferentiated precursors expressing the dorsal forebrain marker PAX6 (Fig. 1a **middle**). After 43 of differentiation *in vitro* days significant numbers of cells expressing the cortical marker DCX (Supplementary Fig. 3) and the mature form of MAP2 were observed in the cultures (Fig. 1a **lower**). Five independent differentiations were performed with four control lines, four TS lines, one 22q11 deletion syndrome line, and one human ESC line (H9). Each line was differentiated at least twice. In addition, two more control lines and one TS line were used for the rescue experiment (see also Supplementary Table 1). R-roscovitine (Sigma-Aldrich, R7772) was dissolved in DMSO. Neuronal cultures were treated with roscovitine or with the same volume of DMSO at day 39 and day 41. Analyses of neuronal cultures were performed at day 43 of differentiation.

Calcium Imaging

NPCs (at passage two after plating of the neurospheres) or neuronal cultures at day 43 of differentiation, were loaded with 1 μM Fura-2 acetoxymethyl ester (Invitrogen) for 30 min at 37°C in Neurobasal/B27 media, washed with Tyrode's solution, and placed in a perfusion chamber on the stage of an inverted fluorescence microscope (TE2000U; Nikon). Cells were stimulated with high KCl Tyrode's solution (67 mM NaCl, 67 mM KCl for neurons and 100 mM for NPCs, 2 mM $CaCl_2$, 1 mM $MgCl_2$, 30 mM glucose, and 25 mM Hepes, pH 7.4) without or with nimodipine (final concentration 5 μM). Imaging was performed at room temperature on an epifluorescence microscope equipped with an excitation filter wheel and an automated stage. Openlab software (PerkinElmer) software was used to collect and

quantify time-lapse excitation ratio images. Fluorescence images were analyzed using IGOR Pro software (WaveMetrics) software.

Single cell qPCR

Neuronal cultures at day 45 of differentiation were rinsed with HBSS and incubated with Accutase (StemCell Technologies). After one wash with fresh Neurobasal medium (Invitrogen), cells were resuspended in Neurobasal/B27 medium containing $1\mu g\ ml^{-1}$ propidium-iodide (Molecular Probes) and filtered through a 40 μm nylon cell strainer (BD Biosciences). Clone sorting in 96-well qPCR plates (Eppendorf) was performed at the Stanford Shared FACS Facility on a BD Influx cell sorter. Cells were sorted into 10 μl pre-amplification mix containing 40 nM of all primers for the 96 genes of interest, and the following components of the CellsDirect One-Step qRT-PCR Kit (Invitrogen): 2× Reaction Mix, SuperScript III RT/Platinum Taq Mix. After sorting, samples were reverse transcribed and pre-amplified for 18 cycles. Pre-amplified samples were diluted (2×) with TE buffer and stored at −20°C. Sample and assay (primer pairs) preparation for 96.96 Fluidigm Dynamic arrays was done according to the manufacturer's recommendation. Briefly, the sample was mixed with 20× DNA Binding Dye Sample Loading Reagent (Fluidigm Corp.), 20× EvaGreen (Biotium) and TaqMan® Gene Expression Master Mix (Applied Biosystems). Assays were mixed with 2× Assay loading reagent (Fluidigm Corp.) and TE to a final concentration of 5 μM. The 96.96 Fluidigm Dynamic Arrays (Fluidigm Corp.) were primed and loaded on an IFC Controller HX (Fluidigm Corp.) and qPCR experiments were run on a Biomark System for Genetic Anaylsis (Fluidigm Corp.). See Supplementary Methods for details on analysis.

Microarrays

RNA from fibroblasts, iPSCs, NPCs, neurons at rest or neurons stimulated with KCl (day 43 of differentiation), was isolated using the RNeasy Mini kit and the RNase-Free DNase set (Qiagen). Total RNA (200 ng) was amplified, labeled, and hybridized on Illumina HumanRef-8 v3 Expression BeadChips (Illumina Inc, San Diego, CA) according to the manufacturer's protocol. Data analysis was performed using the Lumi R[37] and Bioconductor (www.bioconductor.org) packages, as we have previously shown[38]. Briefly, absolute expression values were log2 transformed and normalized using quantile normalization. Data quality control measures included inter-array Pearson correlation, clustering based on most variable genes (coefficient of variance > 0.05), and detection of outlier arrays, as well as probe detection (P values < 0.05). Differential expression analysis was performed using Significance analysis of Microarrays (http://www-stat.stanford.edu/~tibs/SAM/). The statistical criteria for differential expression were FDR < 0.05 and fold change > 1.3. Microarray data is available at GEO (accession code GSE25542).

Supplementary Material

Refer to Web version on PubMed Central for supplementary material.

Acknowledgements

REFERENCES

1. Splawski I, et al. Ca(V)1.2 calcium channel dysfunction causes a multisystem disorder including arrhythmia and autism. Cell. 2004; 119:19–31. [PubMed: 15454078]

2. Yarotskyy V, et al. Roscovitine binds to novel L-channel (CaV1.2) sites that separately affect activation and inactivation. J Biol Chem. 2010; 285:43–53. [PubMed: 19887376]

3. Yarotskyy V, Elmslie KS. Roscovitine, a cyclin-dependent kinase inhibitor, affects several gating mechanisms to inhibit cardiac L-type (Ca(V)1.2) calcium channels. Br J Pharmacol. 2007; 152:386–395. [PubMed: 17700718]

4. Wang X, et al. Phospholemman modulates the gating of cardiac L-type calcium channels. Biophys J. 2010; 98:1149–1159. [PubMed: 20371314]

5. Wang K, et al. Common genetic variants on 5p14.1 associate with autism spectrum disorders. Nature. 2009; 459:528–533. [PubMed: 19404256]

6. Moskvina V, et al. Gene-wide analyses of genome-wide association data sets: evidence for multiple common risk alleles for schizophrenia and bipolar disorder and for overlap in genetic risk. Mol Psychiatry. 2009; 14:252–260. [PubMed: 19065143]

7. Nyegaard M, et al. CACNA1C (rs1006737) is associated with schizophrenia. Mol Psychiatry. 2010; 15:119–121. [PubMed: 20098439]

8. Dolmetsch RE, Pajvani U, Fife K, Spotts JM, Greenberg ME. Signaling to the nucleus by an L-type calcium channel-calmodulin complex through the MAP kinase pathway. Science. 2001; 294:333–339. [PubMed: 11598293]

9. Barrett CF, Tsien RW. The Timothy syndrome mutation differentially affects voltage- and calcium-dependent inactivation of CaV1.2 L-type calcium channels. Proc Natl Acad Sci U S A. 2008; 105:2157–2162. [PubMed: 18250309]

10. Takahashi K, Yamanaka S. Induction of pluripotent stem cells from mouse embryonic and adult fibroblast cultures by defined factors. Cell. 2006; 126:663–676. [PubMed: 16904174]

11. Yu J, et al. Induced pluripotent stem cell lines derived from human somatic cells. Science. 2007; 318:1917–1920. [PubMed: 18029452]

12. Yazawa M, et al. Using induced pluripotent stem cells to investigate cardiac phenotypes in Timothy syndrome. Nature. 2011; 471:230–234. [PubMed: 21307850]

13. Zhang SC, Wernig M, Duncan ID, Brustle O, Thomson JA. In vitro differentiation of transplantable neural precursors from human embryonic stem cells. Nat Biotechnol. 2001; 19:1129–1133. [PubMed: 11731781]

14. Pankratz MT, et al. Directed neural differentiation of human embryonic stem cells via an obligated primitive anterior stage. Stem Cells. 2007; 25:1511–1520. [PubMed: 17332508]

15. Li XJ, et al. Coordination of sonic hedgehog and Wnt signaling determines ventral and dorsal telencephalic neuron types from human embryonic stem cells. Development. 2009; 136:4055–4063. [PubMed: 19906872]

16. Warren L, Bryder D, Weissman IL, Quake SR. Transcription factor profiling in individual hematopoietic progenitors by digital RT-PCR. Proc Natl Acad Sci U S A. 2006; 103:17807–17812. [PubMed: 17098862]

17. Flatz L, et al. Single-cell gene-expression profiling reveals qualitatively distinct CD8 T cells elicited by different gene-based vaccines. Proc Natl Acad Sci U S A. 2011

18. Qin J, Mizuguchi M, Itoh M, Takashima S. Immunohistochemical expression of doublecortin in the human cerebrum: comparison of normal development and neuronal migration disorders. Brain Res. 2000; 863:225–232. [PubMed: 10773210]

19. Garbelli R, et al. Layer-specific genes reveal a rudimentary laminar pattern in human nodular heterotopia. Neurology. 2009; 73:746–753. [PubMed: 19535771]

20. Saito T, et al. Neocortical Layer Formation of Human Developing Brains and Lissencephalies: Consideration of Layer-Specific Marker Expression. Cereb Cortex. 2010

21. Alcamo EA, et al. Satb2 regulates callosal projection neuron identity in the developing cerebral cortex. Neuron. 2008; 57:364–377. [PubMed: 18255030]

22. Britanova O, et al. Satb2 is a postmitotic determinant for upper-layer neuron specification in the neocortex. Neuron. 2008; 57:378–392. [PubMed: 18255031]

23. Leone DP, Srinivasan K, Chen B, Alcamo E, McConnell SK. The determination of projection neuron identity in the developing cerebral cortex. Curr Opin Neurobiol. 2008; 18:28–35. [PubMed: 18508260]

24. Pinto D, et al. Functional impact of global rare copy number variation in autism spectrum disorders. Nature. 2010; 466:368–372. [PubMed: 20531469]

25. Garbett K, et al. Immune transcriptome alterations in the temporal cortex of subjects with autism. Neurobiol Dis. 2008; 30:303–311. [PubMed: 18378158]

26. Ip BK, Bayatti N, Howard NJ, Lindsay S, Clowry GJ. The corticofugal neuron-associated genes ROBO1, SRGAP1, and CTIP2 exhibit an anterior to posterior gradient of expression in early fetal human neocortex development. Cereb Cortex. 2011; 21:1395–1407. [PubMed: 21060114]

27. Romano G, Suon S, Jin H, Donaldson AE, Iacovitti L. Characterization of five evolutionary conserved regions of the human tyrosine hydroxylase (TH) promoter: implications for the engineering of a human TH minimal promoter assembled in a self-inactivating lentiviral vector system. J Cell Physiol. 2005; 204:666–677. [PubMed: 15744773]

28. Raghanti MA, et al. Species-specific distributions of tyrosine hydroxylase-immunoreactive neurons in the prefrontal cortex of anthropoid primates. Neuroscience. 2009; 158:1551–1559. [PubMed: 19041377]

29. Yarotskyy V, Gao G, Peterson BZ, Elmslie KS. The Timothy syndrome mutation of cardiac CaV1.2 (L-type) channels: multiple altered gating mechanisms and pharmacological restoration of inactivation. J Physiol. 2009; 587:551–565. [PubMed: 19074970]

30. Barttfeld P, et al. A big-world network in ASD: Dynamical connectivity analysis reflects a deficit in long-range connections and an excess of short-range connections. Neuropsychologia. 2011; 49:254–263. [PubMed: 21110988]

31. Geschwind DH, Levitt P. Autism spectrum disorders: developmental disconnection syndromes. Curr Opin Neurobiol. 2007; 17:103–111. [PubMed: 17275283]

32. Casanova MF, et al. Reduced gyral window and corpus callosum size in autism: possible macroscopic correlates of a minicolumnopathy. J Autism Dev Disord. 2009; 39:751–764. [PubMed: 19148739]

33. D'Souza A, Onem E, Patel P, La Gamma EF, Nankova BB. Valproic acid regulates catecholaminergic pathways by concentration-dependent threshold effects on TH mRNA synthesis and degradation. Brain Res. 2009; 1247:1–10. [PubMed: 18976638]

34. Toru M, Nishikawa T, Mataga N, Takashima M. Dopamine metabolism increases in post-mortem schizophrenic basal ganglia. J Neural Transm. 1982; 54:181–191. [PubMed: 6127373]

35. Elkabetz Y, et al. Human ES cell-derived neural rosettes reveal a functionally distinct early neural stem cell stage. Genes Dev. 2008; 22:152–165. [PubMed: 18198334]

36. Tole S, Patterson PH. Regionalization of the developing forebrain: a comparison of FORSE-1, Dlx-2, and BF-1. J Neurosci. 1995; 15:970–980. [PubMed: 7869122]

37. Du P, Kibbe WA, Lin SM. lumi: a pipeline for processing Illumina microarray. Bioinformatics. 2008; 24:1547–1548. [PubMed: 18467348]

38. Coppola G, et al. Gene expression study on peripheral blood identifies progranulin mutations. Ann Neurol. 2008; 64:92–96. [PubMed: 18551524]

39. Dulcis D, Spitzer NC. Illumination controls differentiation of dopamine neurons regulating behaviour. Nature. 2008; 456:195–201. [PubMed: 19005547]
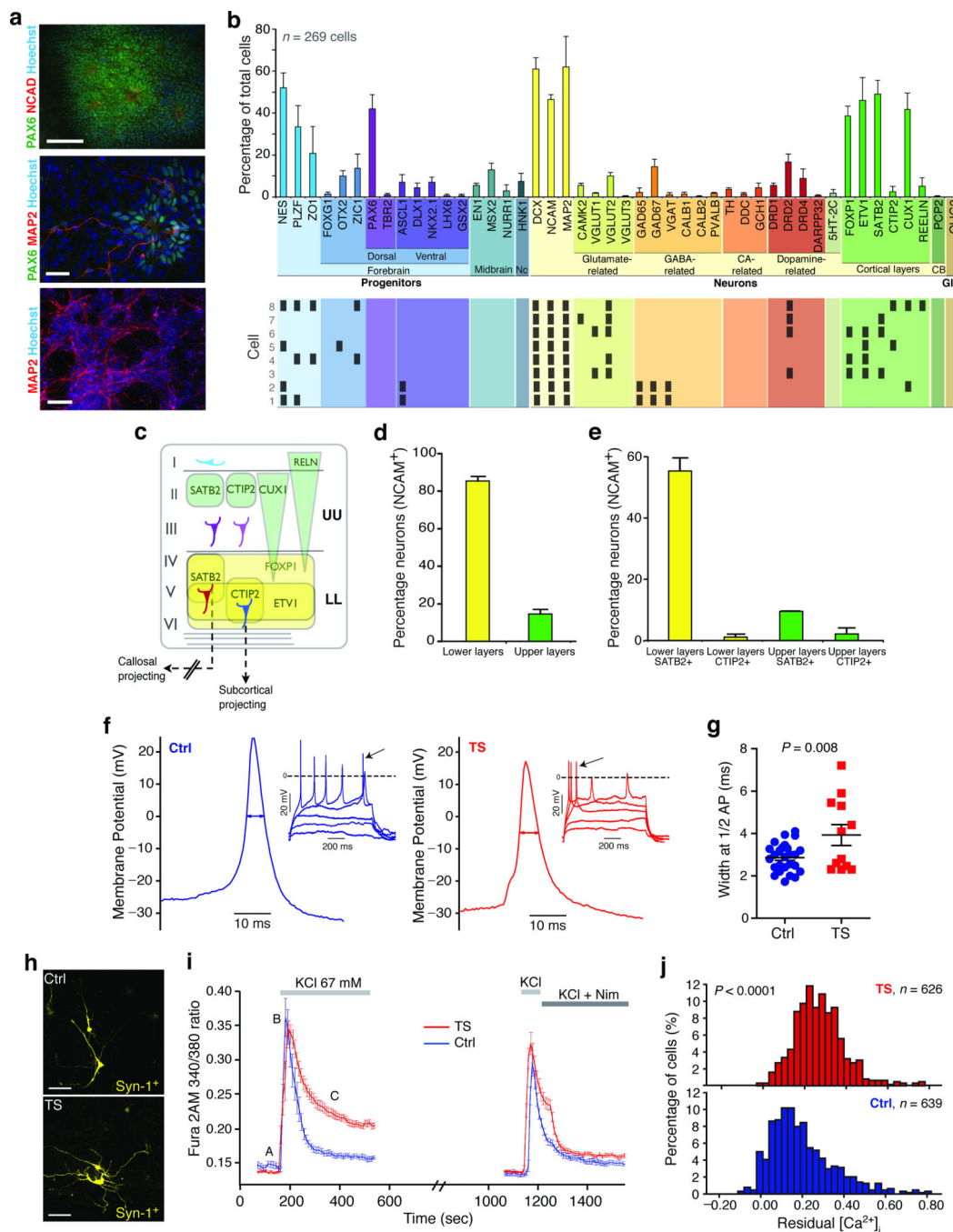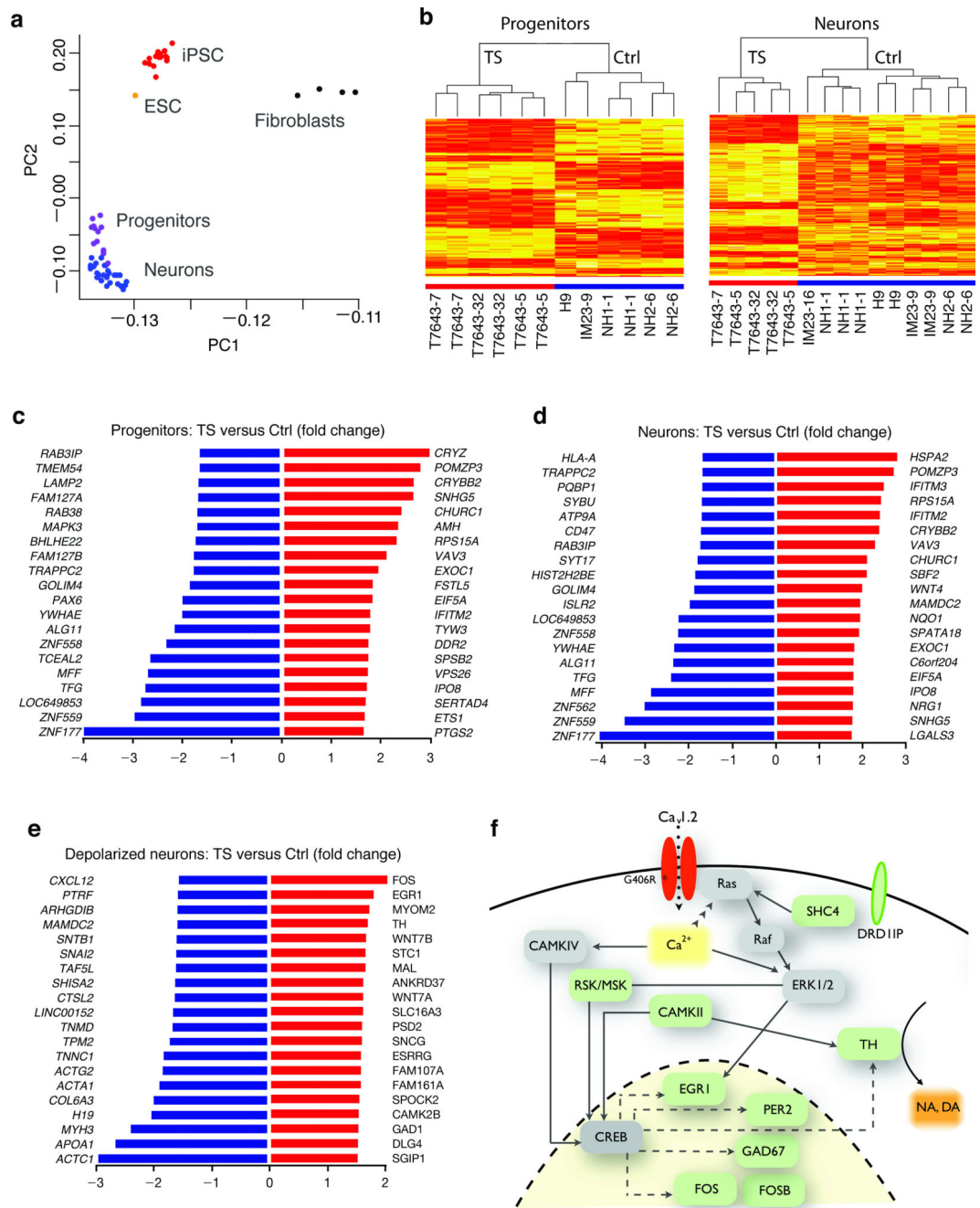
Figure 1. Characterization of iPSC-derived NPCs and neurons

(**a**) Immunostaining of neural rosettes (upper: PAX6, N-Cadherin, Hoescht; scale bar is 100 μm), neurons (MAP2) and progenitors (PAX6) after plating of the neurospheres (middle, scale bar 100 μm) and cultures at day 43 of differentiation (lower: MAP2, Hoescht; scale bar is 200 μm). The middle image is from a Timothy syndrome–derived culture, and the other two are from cultures derived from control individuals. (**b**) Single cell gene expression analysis (Fluidigm) of the population of cells at 45 days of differentiation. Shown are the proportion of cells that express a cell-specific marker (mean ± s.e.m.; *n* = 269 cells from

three control iPSC lines). The lower panel shows gene expression profiles of single neurons. (**c**) Scheme illustrating marker gene expression in upper and lower layers of the human cortex. (**d**) Fraction of neurons ($NCAM^+$) expressing lower ($FOXP1^+/ETV1^+$) or upper layer ($FOXP1–/ETV1–$) cortical markers as assessed by Fluidigm (mean ± s.e.m; $n = 116$ cells from three controls iPSC lines). (**e**) Fraction of subpopulations of upper and lower layer neurons ($NCAM^+$) expressing $CTIP2$ or $SATB2$. (**f**) Representative current clamp recordings (holding potential −65 mV; 1s current pulses, $I_{inj} = 5–10$ pA) from TS and control derived neurons. (**g**) APs recorded from TS neurons were significantly wider. (**h**) Representative images of control and TS neurons expressing YFP under the control of the Synapsin-1 promoter (scale bars are 50 μm). (**i**) Average $[Ca^{2+}]_i$ measurements in Synapsin-1 expressing neurons depolarized twice with 67 mM KCl and treated with 5 μM nimodipine (TS; $n = 10$ neurons; Ctrl; $n = 9$ neurons). (**j**) Histogram of residual $[Ca^{2+}]_i$ ($[C–A]/[B–A]$) in neurons (three TS lines, three control lines, t-test, $P < 0.0001$; see also Supplementary Fig. 8c).
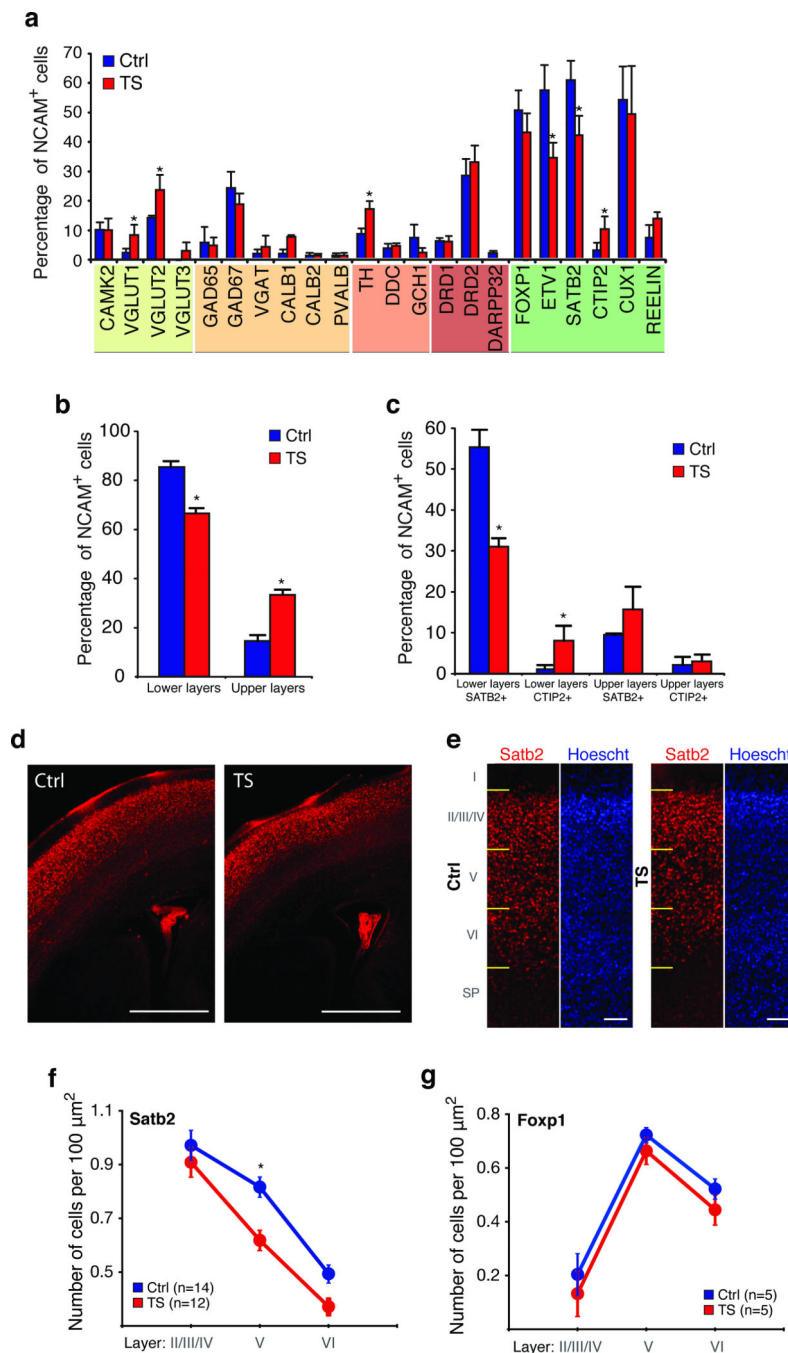
Figure 2. Characterization of NPCs and neurons derived from TS individuals and controls by genome-wide microarrays

(**a**) Principal component analysis of whole-genome gene expression profiles for fibroblasts, iPSC, embryonic stem cells (ESC), NPCs and neurons showing clustering of cell types based on the first two principal components (PC1 and PC2). (**b**) Heatmaps depicting expression levels of genes differentially expressed between TS and control NPCs and neurons. Each column represents an independent differentiation of an iPSC line. Genes that are highly expressed in TS cells relative to controls are shown in red. Dendrograms show

hierarchical clustering of samples based on differentially expressed genes. (**c**) and (**d**) List of top 20 genes showing the highest expression differences between TS and control cells (**c**, progenitors; **d**, neurons). (**e**) Differentially expressed genes in TS neurons relative to control neurons after electrical stimulation. (**f**) Scheme illustrating interactions between a subset of calcium regulated genes upregulated in TS (shown in green).

Figure 3. Characterization of neuronal subpopulations differentiated from TS and control iPSCs
(**a**) Single cell qPCR analysis (Fluidigm) showing the proportion (mean ± s.e.m., *$P < 0.05$, Chi-square test) of *NCAM*+ neurons expressing subtype-specific markers, for control ($n = 125$ cells, three lines) and TS cultures ($n = 140$ cells, three lines). (**b**) Fraction of neurons expressing upper and lower cortical layer makers in TS ($n = 125$ cells) and control cortical cultures ($n = 116$ cells; mean ± s.e.m. *$P < 0.05$, Chi-square test). (**c**) Fraction of neurons expressing *SATB2* and *CTIP2* and either lower or upper layer cortical markers in TS and control cultures (mean ± s.e.m. *$P < 0.05$, Chi-square test). (**d**) 50× image of Satb2 stained

cortical sections from a control mouse and a mouse expressing the TS channel in the forebrain showing a decrease in Satb2$^+$ cells. Scale bar is 500 μm. (**e**) Image of Satb2 stained cortical sections from control and TS mouse at P0.5 (scale bar is 50 μm). (**f**) Measurement of the number of Satb2$^+$ cortical neurons in cortical sections from TS and control mice (mean ± s.e.m.; TS: $n = 12$ animals, Ctrl: $n = 14$ animals; two-way ANOVA, $P = 0.001$; asterisk denotes $P < 0.05$ for posthoc analysis) (**g**) Distribution of Foxp1$^+$ neurons in cortical sections from TS and control mice (mean ± s.e.m.; $n = 5$ animals per group; two-way ANOVA, $P > 0.05$).
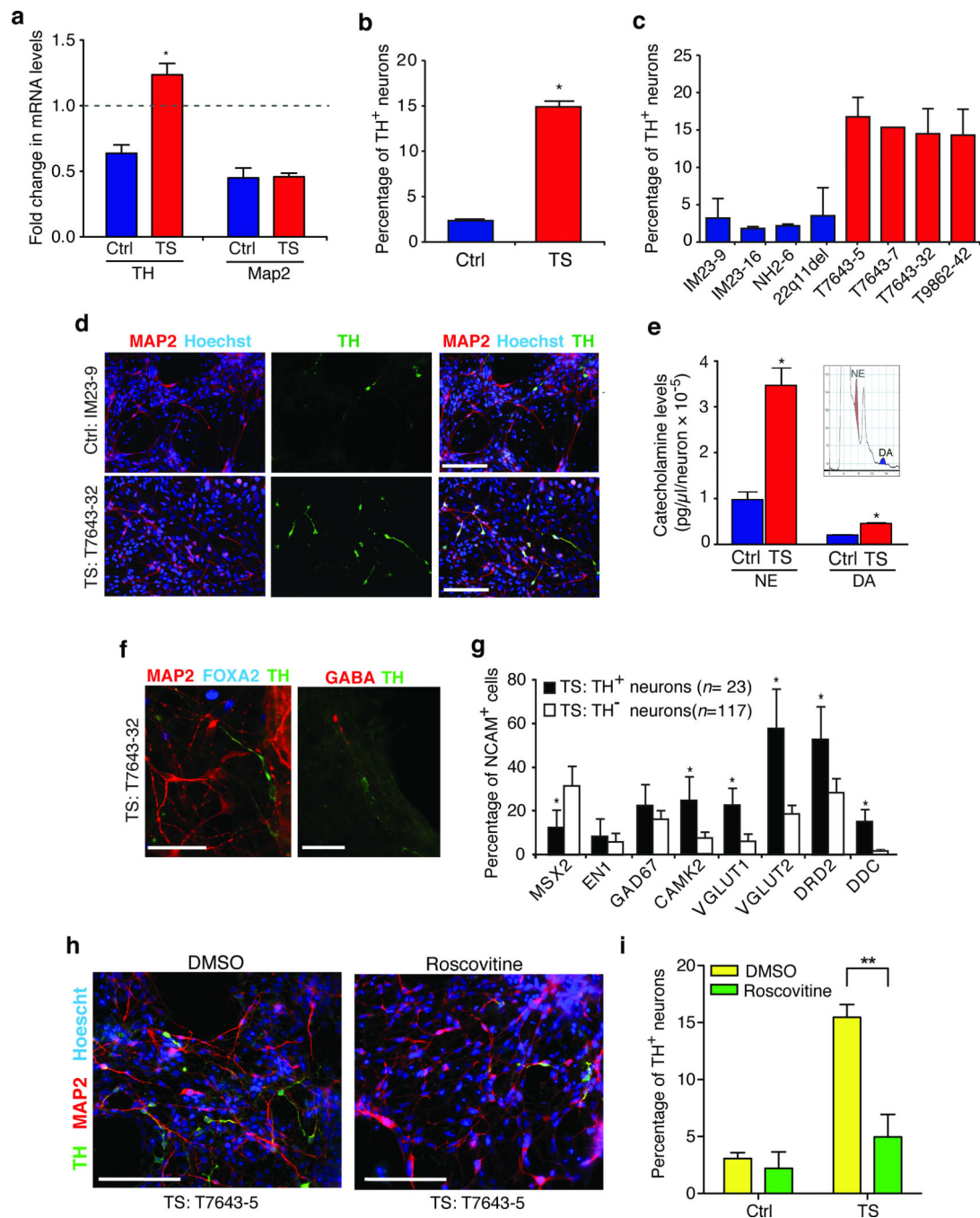
Figure 4. Abnormal expression of TH in neurons from TS individuals

(**a**) Fold changes in *TH* and *MAP2* mRNA levels in TS and control neurons after nine hours of depolarization with 67 mM KCl. (**b**) TS neuronal cultures contain an excess number of TH+ neurons (*$P < 0.001$, t-test). (**c**) The proportion of TH+ neurons (TH+/MAP2+) is shown for three control lines from two healthy individuals (IM23-9, IM23-16, NH2-6), one line derived from a individual with 22q11.2 deletion syndrome, and four TS lines from two individuals (T7643-5, T7643-7, T7643-32, T9862-42). (**d**) Representative images of neurons stained with TH and MAP2 specific antibodies and Hoechst 33258 (scale bars are 200 μm).

(**e**) Norepinephrine (NE, *P = 0.004) and dopamine (DA, *P = 0.001) levels are elevated in media collected from TS neuronal cultures relative to controls. Inset shows an HPLC chromatogram with the peaks for NE and DA. (**f**) TH$^+$ neurons (green) in TS cultures (T7643-32 line is shown) are not immunostained by antibodies to FOXA2 (left, blue) or GABA (right, red). Scale bar is 50 μm. (**g**) Fraction of TH$^+$ or TH$^-$ neurons from TS individuals that co-express other neuronal marker genes (mean ± s.e.m.,* $P < 0.05$, Chi-square test). (**h**) Cultures of TS neurons treated with roscovitine (15 μM at day 39 and 10 μM at day 41) or DMSO and stained with TH and MAP2 specific antibodies at day 43 of differentiation. Scale bar is 200 μm. (**i**) Proportion of TH$^+$ neurons (TH$^+$/MAP2$^+$) in control and TS cultures after treatment with roscovitine or DMSO (mean ± s.e.m., two-way ANOVA, **$P < 0.001$).